

## Supporting Information for:

### Attachment/detachment hysteresis of the fiber-based magnetic grabbers

Yu Gu<sup>a</sup> and Konstantin G. Kornev<sup>\*a</sup>

<sup>a</sup> Department of Materials Science and Engineering, Clemson University, Clemson, SC 20634

#### 1 Magnetic field distribution

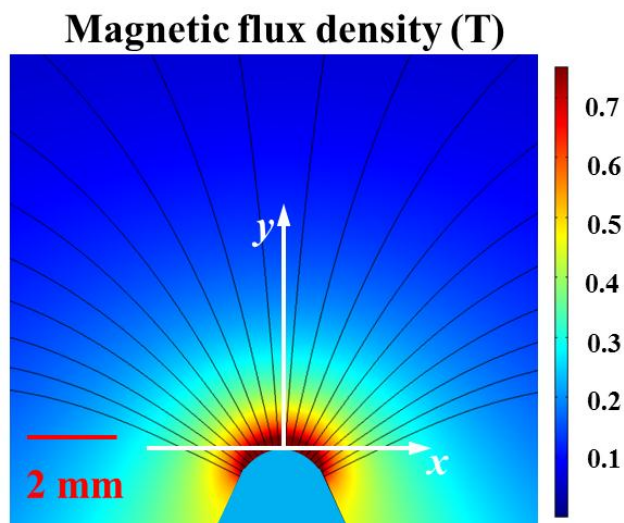


Figure 1 Coordinate system with respect to magnet and the field distribution in the vicinity of magnet simulated from COMSOL after calibration with glass fiber.

In the region  $0 < x < 1$  mm,  $-0.5 < y < 2$  mm, the magnitude of magnetic field can be well approximated by the following function,:

$$B(x, y) \approx \frac{B_0}{[f(\alpha_m x) \cdot \alpha_m y + g(\alpha_m x)]^2} \begin{cases} f(\alpha_m x) = -0.18(\alpha_m x)^2 + 0.028(\alpha_m x) + 0.47 \\ g(\alpha_m x) = 0.34(\alpha_m x)^2 - 0.024(\alpha_m x) + 1.09 \end{cases} \quad (1)$$

Both coordinates are normalized by the curvature of the magnet pole  $\alpha_m = 1000 \text{m}^{-1}$ . Magnetic field right at the magnet pole was obtained as  $B_0 = 1.1 \text{T}$  is.

The coefficients for the polynomial functions  $f(\alpha_m x)$  and  $g(\alpha_m x)$  were estimated through the following procedures. First, the x-coordinate was fixed and parameters  $f(\alpha_m x)$  and  $g(\alpha_m x)$  were taken as the adjustable ones. These parameters  $f(\alpha_m x)$  and  $g(\alpha_m x)$  were found by fitting the magnetic field with Eq.(1). Repeating this step for different  $x$ , we obtained a series of  $f(\alpha_m x)$ ,

$g(\alpha_m x)$ . Then, these two data sets were fitted with the second order polynomial to determine all the coefficients.

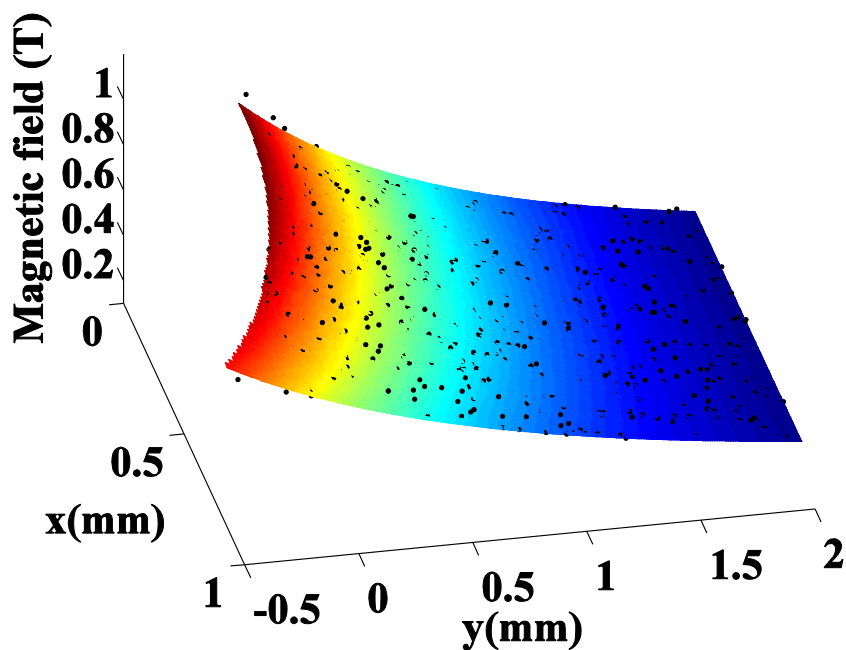


Figure 2 Magnetic field distribution. Black points are the simulation results from COMSOL after a calibration with glass fiber. Colored surface represents Eq. (1)

Figure 2 shows the magnetic field distribution. Black points are the simulated ones with COMSOL after the calibration with glass fiber. The colored surface calculated with Eq.(1) agrees well with the field obtained from the FEM calibration.

## 2 Magnetic force applied to the droplet

### 2.1 Direction of magnetic force

The magnetic moment of droplet is measured by AGM 2900 and the relation follows the Langevin function:

$$m(B) = \alpha \left[ \cot(\beta B) - \frac{1}{\beta B} \right] \quad \alpha = N\mu, \beta = \frac{\mu}{k_B T} \quad (2)$$

The magnetic force can be determined by combining eq.(1) and the following equations:

$$\begin{cases} F_x = m_x \frac{\partial}{\partial x} B(x, y) \\ F_y = m_y \frac{\partial}{\partial y} B(x, y) \end{cases} \quad (3)$$

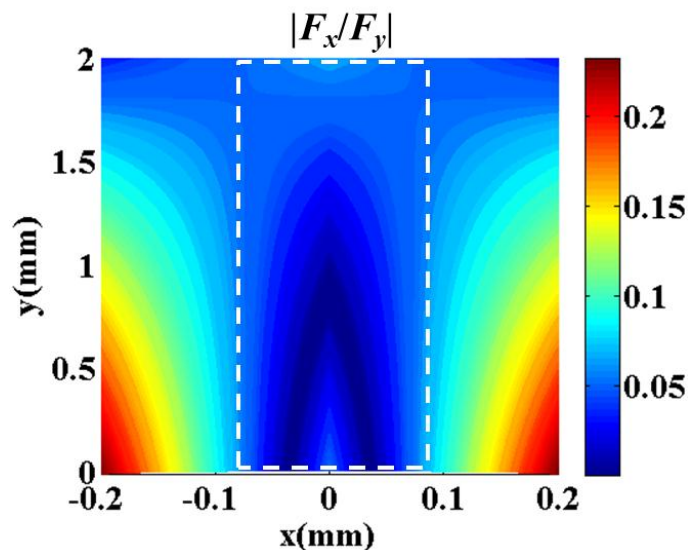


Figure 3 The ratio between x-component and y-component of the magnetic force. Our experiment is conducted within the region bounded by the dashed rectangle

Figure 3 shows the  $F_x / F_y$  ratio in the vicinity of the magnet pole. Our experiments were conducted within the region bounded by the dashed rectangle. In this region, the ratio  $|F_x/F_y|$  was less than 0.05. Therefore, for the interpretation of our experiments, it was safe to ignore the x-component of magnetic force.

## 2.2 Magnitude of magnetic force along the y-axis

The magnetic force along the y-axis was calculated by Eq.(3). It can be well approximated by the following equation:

$$F_m = \frac{F_0}{(\beta_m y + 1)^3} \quad (4)$$

$\beta_m$  was taken as an adjustable parameter to fit the numerical data points shown in Figure 4. The solid curve shows an excellent match with the numerical data. Hence the dipole-type approximation of magnetic force is applicable for our experiment.

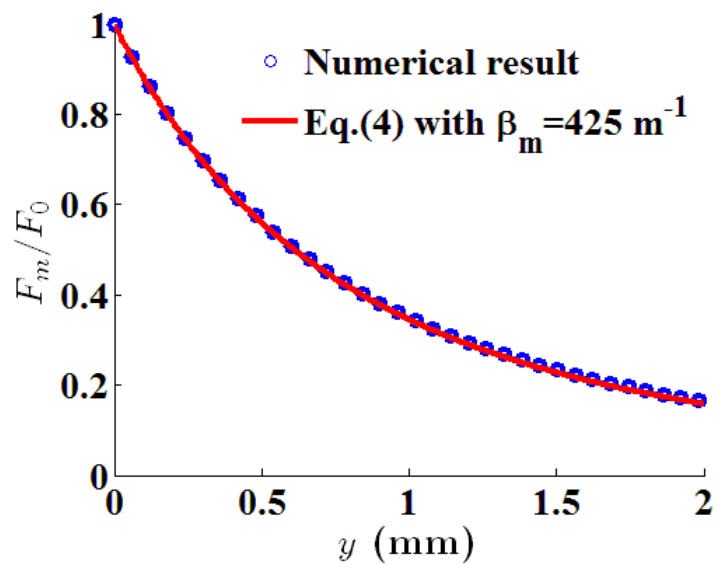


Figure 4 The distribution of magnetic force along the  $y$ -axis. The circles represent the numerical calculations with Eq.(3) and the solid curve corresponds to the fitted curve with Eq.(4)